

## Singular value decomposition of received ultrasound signal for separation of blood flow and cavitation

受信超音波信号の特異値分解による血流とキャビテーションの分離

Hayato Ikeda<sup>1,‡</sup>, Ryo Nagaoka<sup>1</sup>, Maxime Lafond<sup>1</sup>, Shin Yoshizawa<sup>1</sup>, Ryosuke Iwasaki<sup>1</sup>  
 Moe Maeda<sup>1</sup>, Shin-ichiro Umemura<sup>1</sup>, and Yoshihumi Saijo<sup>1</sup> (<sup>1</sup>Tohoku Univ.)  
 池田隼人<sup>1,‡</sup>, 長岡亮<sup>1</sup>, マキシムラフォン<sup>1</sup>, 吉澤晋<sup>1</sup>, 岩崎亮祐<sup>1</sup>, 前田萌<sup>1</sup>, 梅村晋一郎<sup>1</sup>,  
 西條芳文<sup>1</sup> (<sup>1</sup>東北大学)

### 1. Introduction

High-Intensity Focused Ultrasound (HIFU) is noninvasive treatment focusing ultrasound from outside the body to coagulate target tissue by heating it.<sup>1)</sup> In blood-vessel targeting HIFU treatment, cavitation are utilized for enhancing the ultrasonic heating to overcome the cooling effect by the blood flow. In ultrasound enhanced thrombolysis, mechanical action of cavitation is utilized for crushing and tearing the thrombus and delivering the thrombolytic agent into the thrombus.<sup>2)</sup> However, the tissues surrounding the target may be damaged due to excessive cavitation bubbles. A real-time monitoring method to separate blood flow and cavitation is needed to ensure the safety of such treatments.

In this study, we propose a novel filtering method separating blood flow and cavitation signals by employing a singular value decomposition (SVD).

### 2. Materials and Methods

#### 2.1 Experimental setup

**Fig.1** shows a schematic of the experimental setup. HIFU was generated from a 128-ch 2D-array transducer (focal length: 120 mm) at a driving frequency of 1.0 MHz. A sector probe with a center frequency of 3.0 MHz (Hitachi Aloka Medical, UST-52105) was connected to a programmable ultrasound scanner (Vantage256, Verasonics) to acquire RF data for imaging.

#### 2.2 Acquisition of cavitation signal

**Fig.2** shows a sequence of the HIFU insonification and imaging. The intensity and exposure duration of HIFU were 40 kW/cm<sup>2</sup> and 100 μs, respectively. HIFU was irradiated twice at a pulse repetition frequency (PRF) of 50Hz. Between the HIFU insonification, 54 diverging waves were sent at a PRF of 3.0 kHz. One data block for imaging was composed of 18 sets, each consisting of three diverging waves steered at different angles

of -20°, 0°, and 20° for compounding operation, which reduced the frame rate from 3.0 kHz to 1.0 kHz. RF data for 36 frames of images were used for separating signals between blood flow and cavitation.

#### 2.3 Acquisition of blood flow signal

A blood flow phantom (Poly-Vinyl Alcohol) with a 4 mm diameter cylindrical cavity was set at the HIFU geometric focus. A blood mimicking fluid consisting of glycerin 70 wt%, water 30 wt% and godball (ultrasonic scatterer) was flown at a steady velocity of 40 cm/s. RF data were acquired without HIFU insonification.

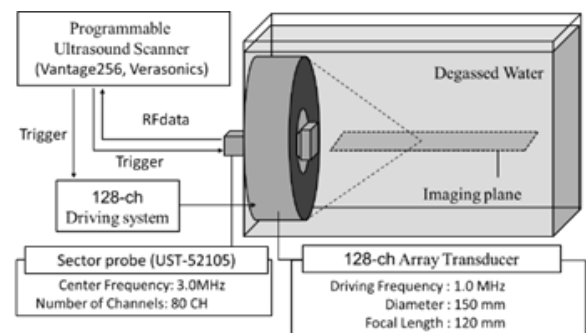


Fig. 1 Schematic of experimental setup

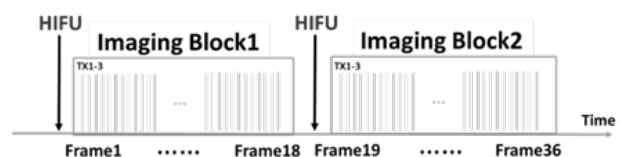


Fig. 2 Sequence of HIFU and imaging

#### 2.4 Signal synthesis and SVD filtering

The signals acquired as described in 2.2 and 2.3 were summed to synthesize the signal including both cavitation and blood flow. It was returned to the programmable ultrasound scanner for image reconstruction. The image data in size of 113×93×36 ( $n_z \times n_x \times n_t$ ) were converted into two-dimensional data  $M$  ( $n_z \cdot n_x \times n_t$ ). The singular

value decomposition can be expressed as

$$M = U\Delta V^* = \sum_{i=1}^{n_t} \lambda_i U_i \otimes V_i^* \quad (1)$$

where  $\Delta$  is a diagonal matrix with dimension  $(n_z \cdot n_x \times n_t)$  containing the ordered singular values  $\lambda_i (i=1, 2, \dots, n_t)$ . The  $U$  and  $V$  are unitary matrices with respective dimensions  $(n_z \cdot n_x \times n_t)$  and  $(n_t \times n_t)$ . The symbol  $*$  stands for the conjugate transpose. By defining two threshold singular values  $\#p$  and  $\#q$ , the filtering can be expressed as

$$M^f = U\Delta^f V^* = \sum_{i=p}^q \lambda_i U_i \otimes V_i^* \quad (2)$$

The singular value selection was automatically performed by a square base 2D fitting algorithm<sup>3)</sup> for a covariance matrix of  $U$  and  $V$ .

### 3. Result and Discussion

**Fig.3** shows a set of spatiotemporal couples vectors of  $U$  and  $V$ . The signal component presumably from the residual microbubbles in the blood flow phantom, that from cavitation, that from mixture between cavitation and blood flow, and that from the blood flow are seen in  $\#1$ ,  $\#2$ ,  $\#20$ , and  $\#36$ , respectively.

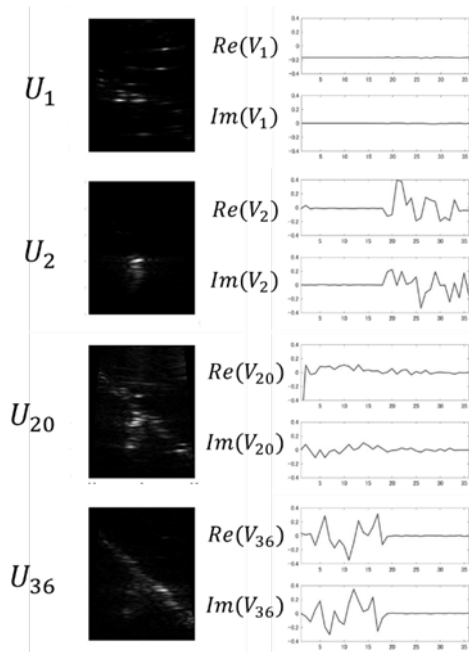


Fig. 3 A set of vectors of  $U$  and  $V$

**Fig.4** shows the covariance matrix of  $U$  and  $V$ , respectively, and the results using the square base 2D fitting algorithm. The cavitation signals had a larger spatial correlation than the blood flow signals. On the other hand, blood flow signals had larger temporal correlation than the cavitation signals due to steady flow. Utilizing the difference in spatiotemporal property, an automatic

thresholding of singular values was tested. **Fig.5** shows the resulting the Power Doppler images, where **(a)** and **(b)** is the cavitation and blood flow image assuming that cavitation and blood flow corresponds to SV of  $\#2$ - $\#19$  and  $\#21$ - $\#36$ , respectively.

In this study, because the cavitation signal was generated in a free fluid, the cavitation bubbles flew due to the acoustic radiation pressure. A noise of cavitation was observed in **Fig5 (b)** as shown white circle. This was because the cavitation signals with the velocity similar to that of the blood flow cannot be separated completely. In the future experiments, a cavitation will be generated in a gel.

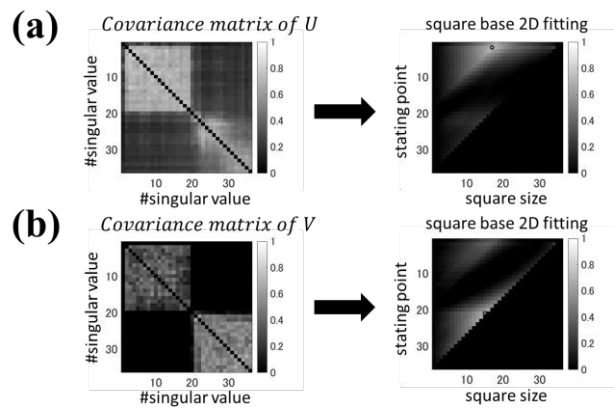


Fig. 4 Covariance matrix, and result of square base 2D fitting algorithm (a)  $U$  (b)  $V$

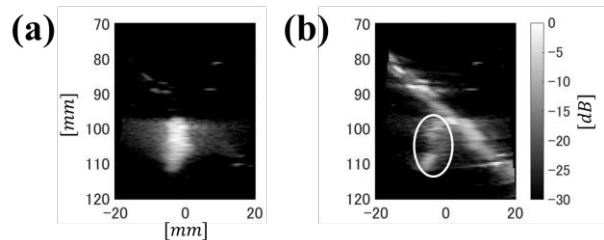


Fig. 5 Power Doppler after SVD filtering (a) Cavitation:  $\#2$  to  $\#19$  (b) Blood flow:  $\#21$  to  $\#36$

### 4. Conclusion

We proposed a filtering method that can separate the blood flow and cavitation components using singular value decomposition. In addition, we investigated an algorithm for automatic selection of threshold values based on the difference of the spatiotemporal properties.

### References

1. S. Umemura et al: Jpn. J. Appl. Phys. **52** (2013) 07HA02.
2. D. Harpaz: Am. Heart. J. **127** (1994) 1211.
3. B. Arnal: Phys. Med. Biol. **62** (2017) 843.